Nuclear Disarmament Verification

Aldridge, Barritt, Christodoulou, Lu,
Moors, Rajroop, Theodorou, Xiao,
Department of Physics and Astronomy,
University College London,
London WC1E 6BT,
United Kingdom

2012 March 06th

Executive summary

The Context

Why do we Verify? We verify to assure confidence. We have a declaration, our verification methods, and our confidence. If we are too intrusive with our verification methods there is the threat of the spread of proliferation information which could in turn lead to a breakdown of the declaration agreements alongside an increased risk of mass devastation. If the verification methods employed are too feeble, the uncertainty in the confidence will be high and inspectors may fail to detect anomalous behaviour in the hosts disarmament activities. This balance is known as the information barrier and it is spawn from the consideration of ratified treaties, the capabilities of the equipment and the feasibility of the procedure. The treaties outline what information should and shouldnt be shared with the inspectors; the equipment and procedure are the technological or economic constraints. *A chart of time, treaty and declaration information or disarmament rates, there should be an inflection at 2002 * Summers treaty review Nicks information barrier in the context of treaty Lukes weapon introduction Jacks confidence in verification

The Process

What do we verify? Lukes weapon introduction Nicks brief overview Ralphs dismantling process Valentinos chain of custody / Containment and surveillance of dismantlement Lukes Blending down

The Methods

How do we verify? Jenelles Passive detection; Gamma signature, Neutron signature Kaijians detection methods; Induced Gamma and Neutron signature Nicks Pit stuffing Lukes blending down

The Technology

What do we use to verify and how does it work? Valentinos Containment and surveillance / Ralphs review of tags and seals tech Kaijians detection methods Jenelles Passive detection Valentinos Muon Tomography

The Conclusion

(What are the Strengths weaknesses opportunities and threats?)

Final Summary

Contents

1 Introduction

1.1 Sample Section

Here is a sample statement.

$$E = \gamma m_0 c^2$$

2 Political Background

2.1 Treaties

3 Detection Schemes

3.1 Passive Detection

3.2 Active Detection

3.3 Muon Tomography

3.3.1 Cosmic Rays

Cosmic rays are a flux of high energy particles that bombard the earths atmosphere. They are produced in other parts of the universe and approximately 98% of these particles are protons or heavier nuclei and 2% are electrons. These cosmic rays collide with air molecules and produce a shower of particles that include protons, neutrons, electrons, positrons, photons, kaons and pions (both neutral and charged). These particles interact by the nuclear and electromagnetic forces to produce additional particles in a cascade process. Pions will interact with air molecules via the strong force but some will spontaneously decay via the weak force into a muon plus a muon neutrino or an anti-muon neutrino. [1]

$$\pi^+ \rightarrow \mu^+ + \overline{\nu}_\mu \tag{1}$$

$$\pi^- \rightarrow \mu^- + \nu_\mu \tag{2}$$

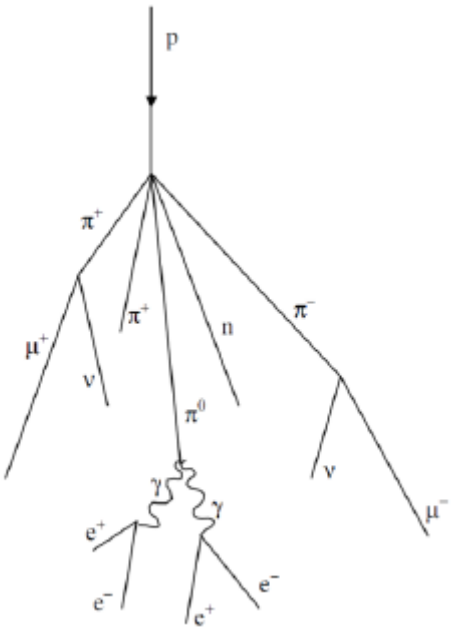

Figure 1: Cosmic ray cascade induced by a cosmic ray proton striking an air molecule nucleus. [1]

3.3.2 Muons

Muons are the most abundant charged particles at sea level. They are produced high in the atmosphere, typically 15 km and lose about 2 GeV before reaching the ground due to ionization. The mean energy of muons at the ground is 4 GeV [2]. They interact with matter via the weak and electromagnetic forces but not with the strong force. They decay via the weak force into an electron plus an electron neutrino or an anti-electron neutrino.

$$\mu^- \rightarrow e^- + \overline{\nu}_e + \nu_\mu \tag{3}$$

$$\mu^+ \rightarrow e^+ + \nu_e + \overline{\nu}_\mu \tag{4}$$

The muon flux at sea level is about 1 muon cm^{-2} min^{-1} [3] or 10000 muons m^{-2} min^{-1}. They are highly penetrating charged radiation. A typical cosmic ray muon of energy 3 GeV can penetrate more than 1000 g cm^{-2} (eg. 10 m of water). As muons pass through matter they either scatter if they have high energy or are absorbed if they have low energy. The angle at which they scatter depends on the atomic number Z (number of protons) of the material. As the atomic number of the material increases, the scattering angle increases. In a layer 10 cm thick, a 3 GeV muon will scatter with an angle of 2.3 mrad in water, 11 mrad in iron and 20 mrad in lead. [4]

3.3.3 Limitations of X-rays

X-ray radiography is successful in many areas but has limitations. X-rays are unable to penetrate dense objects that have a high atomic number. Multiple projections are needed in order to resolve a three-dimensional structure using X-rays and they also pose health risks from radiation. In X-ray radiography, absorption and scattering cause attenuation of the incident beam which determines the intensity of an image pixel. The maximum mean free path of photons is about 25 g cm^{-2} for all materials which corresponds to 2 cm of lead [4]. Even the most penetrating gamma rays are attenuated by an e-folding in 2 cm of lead. A very large incident dose of radiation is needed to penetrate thicker objects and that is harmful for living organisms [5]. A different type of radiography must be used for thicker objects and it must be based on the interaction of charged particles with matter by multiple Coulomb scattering [4].

3.3.4 Muon tomography concept

Muon tomography is based on the multiple Coulomb scattering of muons as they pass through a material. Radiographs of objects of any thickness can be produced by using multiple scattering. Cosmic ray muons are passive and harmless radiation and allow radiograph of dense objects with no artificial dose of radiation such as X-rays or gamma rays. The scattering of muons differs significantly in three different groups of materials: low Z (water, plastic, concrete), medium Z (iron, copper) and high Z (lead, tungsten, uranium) [6]. Each muon carries information about the objects it has penetrated and the properties of these objects can be determined by measuring the scattering of multiple muons. High Z objects can be detected amongst typical low Z and medium Z objects. [3]

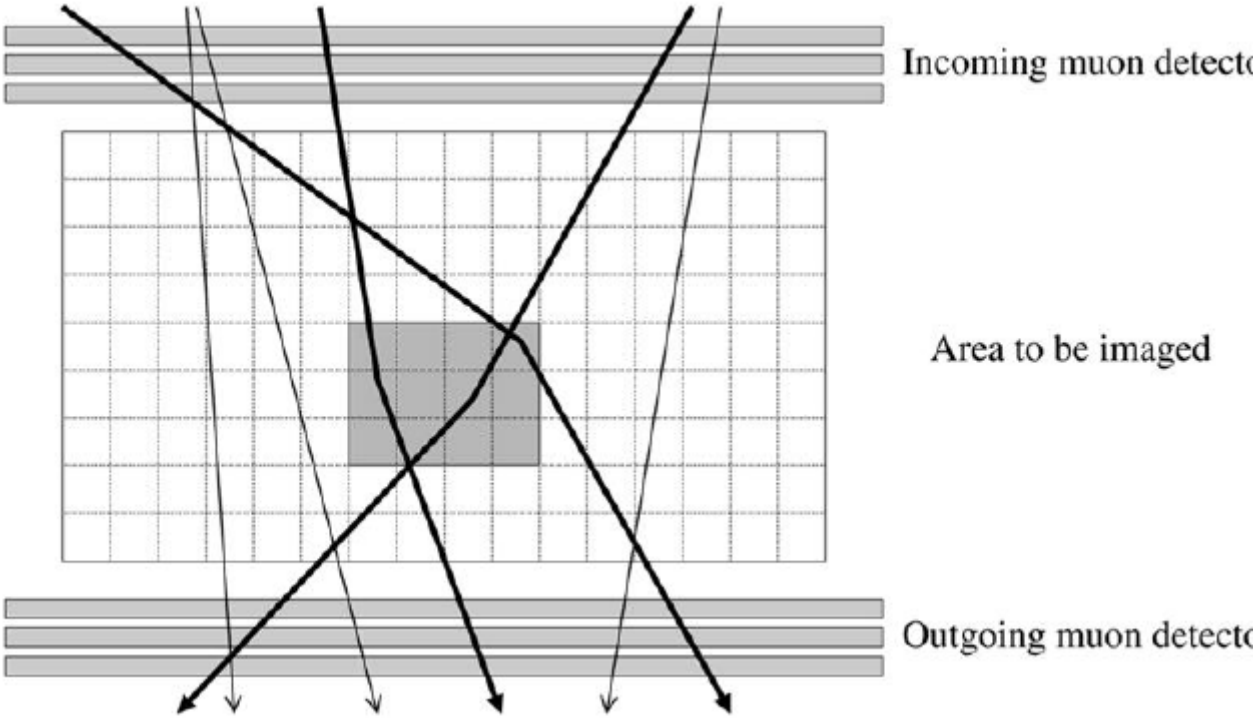

Figure 2: Muon tomography concept. The grey tracks are the muons going through air and the black tracks are the muons that penetrate a dense object. [3]

The muon tomography concept is illustrated above in Figure 2. The position and angle of incoming muon tracks are provided by a set of two or more planes of muon detectors above and below the object. These detectors only detect vertically oriented muons. Side detectors could be used to detect horizontally oriented muons. The detectors above the object measure the position of incident muons in two orthogonal coordinates. The scattering of the muons that pass through the material depends on the type of the object. The detectors below the object measure the positions and angles of the scattered muons. The scattering angle of each muon is calculated from the corresponding incident and scattered measurements. The momentum is calculated from the slight scattering of muons in the detectors themselves. [3]

3.3.5 Simulations of muon tomography

Simulations of muon tomography are very promising and results can be obtained within a very short exposure time of approximately 1 min. The GEANT4 Monte Carlo package is used for the simulations because it implements a complete, accurate and validated model for multiple scattering. A detailed GEANT4 simulation of a passenger van has been produced and reconstruction was achieved using two different methods: mean and median. [3]

The mean method of reconstruction shown on Figure 4 contains red spots

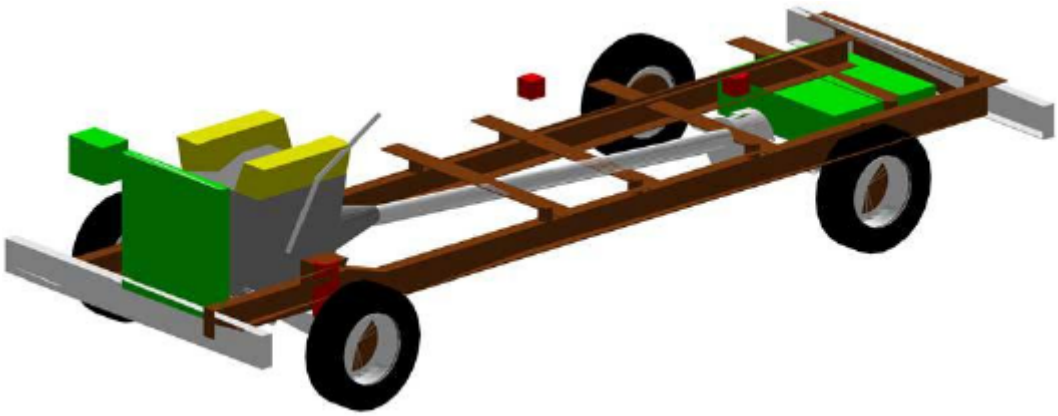

Figure 3: Illustration of major objects in a simulated passenger van using GEANT4. The red block in the centre represents a $10 \times 10 \times 10$ cm^3 solid piece of tungsten which is a high Z threat object. [3]

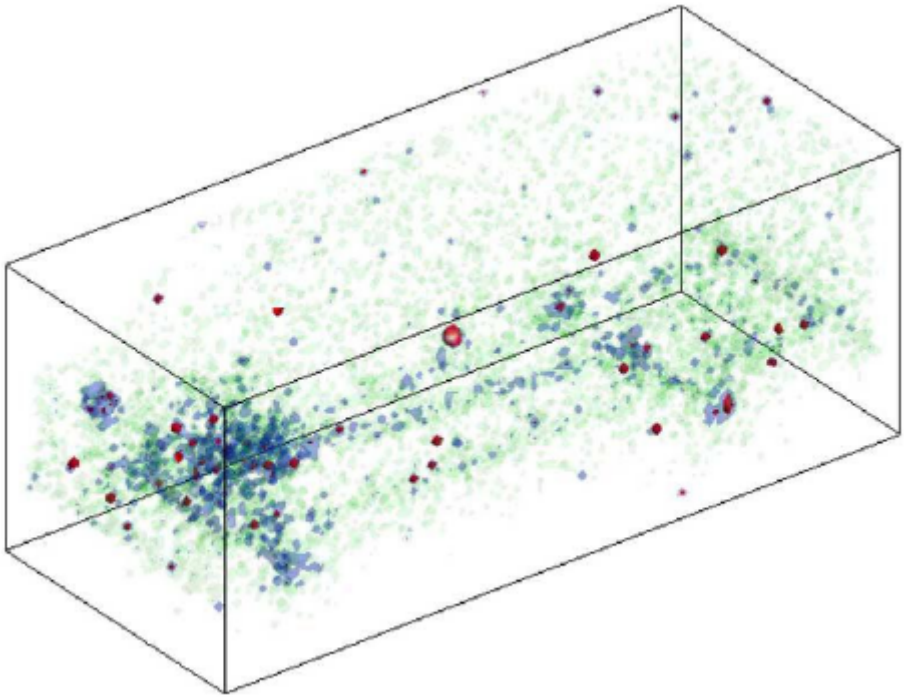

Figure 4: Reconstruction of 1 min of simulation muon exposure of the passenger van using the mean method. [3]

scattered over the image. The median method shown on Figure 5 does not contain these effects. The denser components of the van (engine, battery, drive train) are shown as green (low Z) or blue (medium) but the high Z threat object stands out as red. The median method is clearly better. [3]

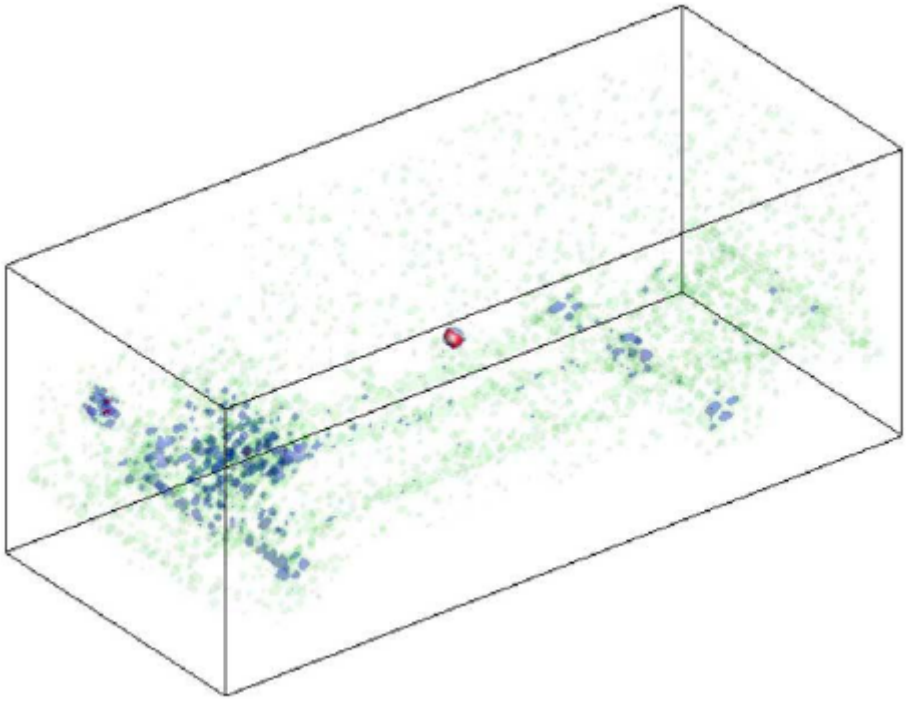

Figure 5: Reconstruction of 1 min of simulation muon exposure of the passenger van using the median method. [3]

A ray crossing algorithm has been developed that highlights locations where strongly scattered muons cross paths. The basis of the ray crossing algorithm is the fact that a high Z object produces many highly scattered rays which intersect in a small volume. A large depth of medium Z material can also produce highly scattered rays but these rays will spread over a larger volume. The algorithm was applied to a simulated scene of a $6 \times 2.4 \times 2.4\ \mathrm{m}^3$ cargo container filled with 12 tons of iron and three $9 \times 9 \times 12\ \mathrm{cm}^3$ uranium bricks were buried within the iron. A cosmic ray exposure of 1 min was simulated and the tracks were processed using the ray crossing algorithm. The results are shown below on Figure 6. [6]

All three uranium bricks are clearly identified on Figure 6a. The image without the uranium bricks is empty of any signal as shown on Figure 6b. The ray crossing algorithm shows great promise in eliminating the scattering background. [6]

Other simulations were also produced using a Monte Carlo simulation code and the results are shown below on Figure 7.

3.3.6 Experimental results of muon tomography

There are a few prototype experimental muon tomography detectors that show excellent results which are consistent with the simulations. A small scale experimental detector system was developed in 2003 at the Los Alamos National

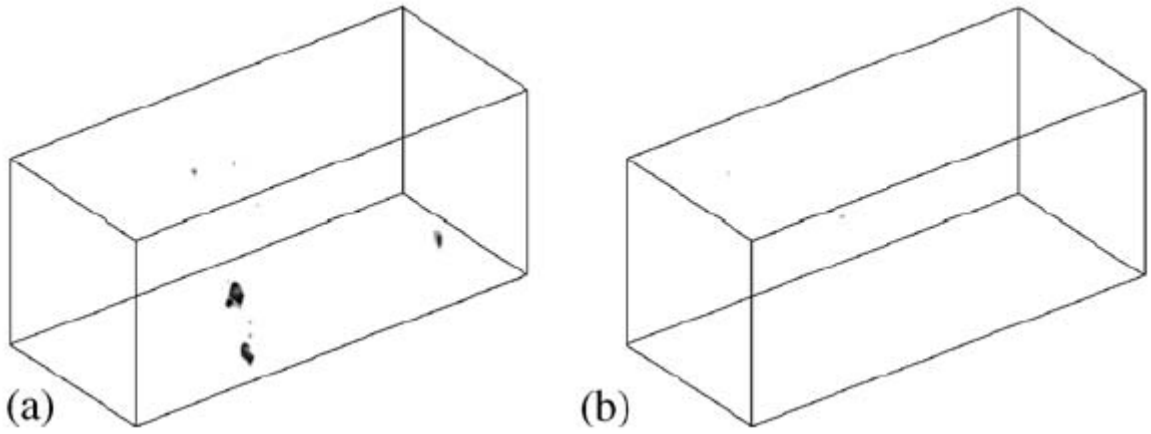

Figure 6: Ray crossing algorithm reconstructions of 1 min of simulated muon radiography of a $6 \times 2.4 \times 2.4$ m^3 cargo container filled with 12 tons of iron and three $9 \times 9 \times 12$ cm^3 uranium bricks (a) and without the uranium bricks (b). [6]

Laboratory, Los Alamos, New Mexico [5]. A picture of the detector is shown below Figure 8.

Eight X and eight Y locations were measured for each muon by four ionizing radiation detectors contained in the detector stack. The two detectors on top measure the incoming muon track while the two detectors at the bottom measure the scattered track. Each delay line drift chamber detector had an active area of 60×60 cm^2. The detector was calibrated with no test object to determine the precision of the position measurement. A Windows based acquisition program was used to collect the data. The reconstruction was approximated using the following simple technique. Multiple scattered tracks were approximated to have only a single scattering event and the point of scatter was located by extrapolating the incident and scattered rays. A maximum likelihood technique was used to assign voxels (3D pixels) to each scattered muon. The reconstructed 3D image of the tungsten test object is shown below on Figure 9. [5]

The data for the above image were collected over several hours because the detector was not fully optimised. An optimised detector with 100% tracking efficiency and large solid angle could acquire the same data in approximately 30 min. The test object and the test support beams can be clearly resolved using this long run. Considerably shorter runs could be used for a simple yes/no detection. [5]

Another sub-scale prototype was built at the Los Alamos National Laboratory in 2006 called the Large Muon Tracker (LMT) which is 20 tall. The design of this detector is very similar to the previous detector. It consists of 6 top and 6 bottom planes of drift tube detectors for each X and Y dimensions (24 planes in total) on a flexible frame. The top and bottom sections are separated by 1.5 m to allow a large sampling region. X and Y tracks are fitted separately to find the slope and intercept of each dimension and combining them yields the 3D trajectory of the muon. A picture of LMT is shown below on Figure 10. [7]

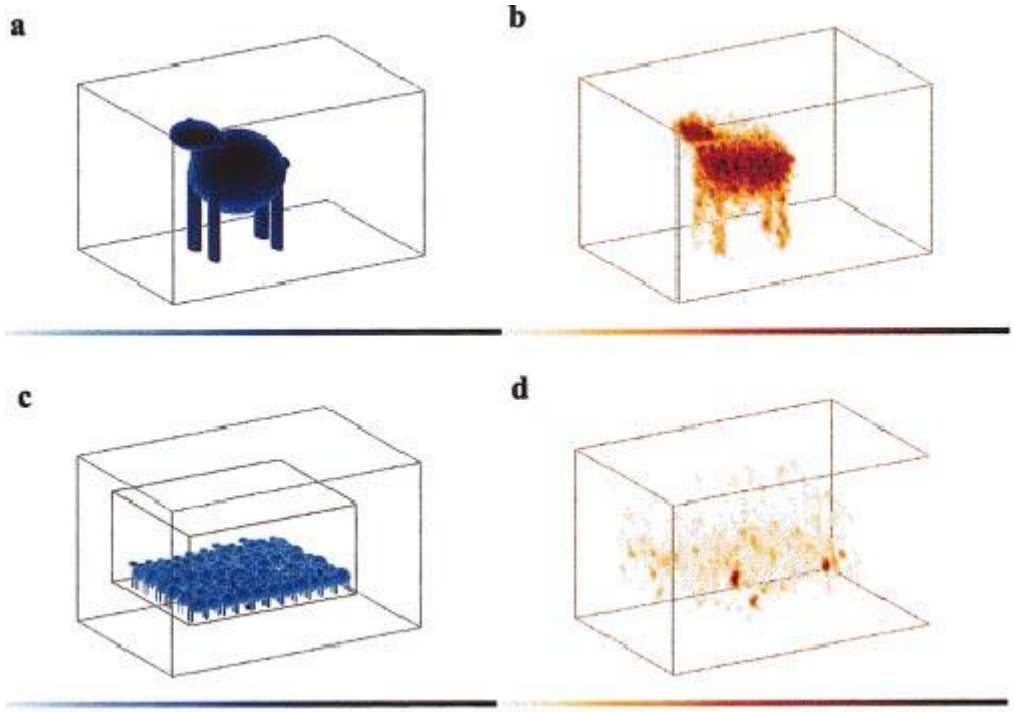

Figure 7: Muon radiograph of a complex target in a volume of $9 \times 3 \times 5.5$ m^3. The first object (a) is a large complex lead sculpture. The reconstructed image (b) shows much of the detail of the object and its based on 1 min of exposure. The second object (c) consists of a $4 \times 2.4 \times 2.4$ m^3 container with walls of thickness equivalent to 3 mm of steel. There are 69 sheep made of water (shown in blue) inside the container with a body size of $60 \times 30 \times 40$ cm^3 and three uranium bricks of size $9 \times 9 \times 12$ cm^3 (shown in black). The reconstructed image (d), based on 1 min of exposure, shows that the 3 uranium bricks stand out. The colour intensity in the two reconstructed images corresponds to the significance of the signal. [5]

The prototype of LMT was completed and tested in 2008. A simple reconstruction technique was used to process the data. The sample volume of $1.5 \times 1.5 \times 1.0$ m^3 was segmented into $2 \times 2 \times 2$ cm^3 voxels. The median scattering angle was calculated for all muons whose trajectories intersected a voxel with an adjustable distance. The prototype was tested using a $10 \times 10 \times 10$ cm^3 lead cube that represented the threat object and it was placed in the LMT along with a car engine and transmission. A photograph of the engine in the LMT is shown below on Figure 11. [8]

Data were collected for approximately 160 min and have been analysed to reconstruct the images shown below on Figure 12. The mean scattering angle is plotted for all trajectories that pass through each voxel. [8]

Another muon tomography prototype is located at the INFN National Laboratories of Legnaro, Padova, Italy. A volume of 11 m^3 can be inspected using the prototype which is ideal for cargo inspection. A picture of the prototype is shown below on Figure 13. [9]

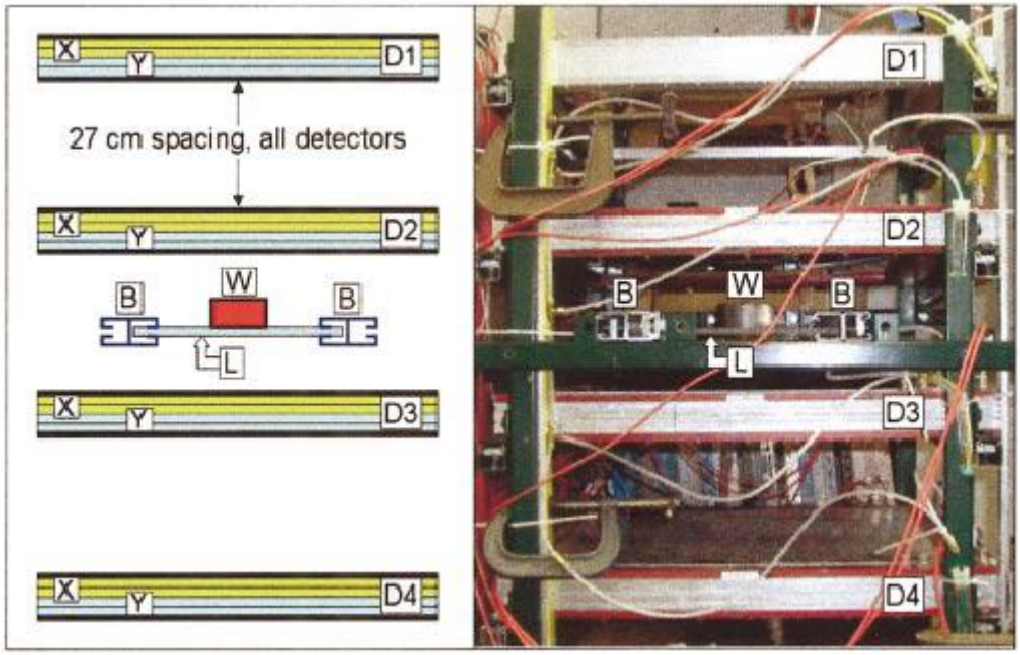

Figure 8: Picture of experimental apparatus at the Los Alamos National Laboratory in 2003. There are four muon detectors labelled D1-D4 with a vertical spacing of 27 cm. The detectors determine the positions and angles of the muons in two orthogonal coordinates (X and Y). The test object (W) was a tungsten cylinder of radius 5.5 cm and height 5.7 cm. A thick Lexan (L) plate of dimensions $35 \times 60 \times 1$ cm^3 and steel support beams (B) were used to support the test object. [5]

Two Muon Barrel drift chambers of dimensions $300 \times 250 \times 29$ cm^3, built for the CMS experiment at CERN, were used for the experiment, separated by 160 cm. A concrete and iron structure is supporting the chambers. There are two additional drift chambers underneath the bottom detector that will be used in the future as a momentum filter. The reconstruction procedure uses a List Mode Iterative Algorithm (LMIA) that process events one at a time instead of grouping similar events together. [9]

The experiment was repeated using two lead blocks of dimensions $10 \times 10 \times 20$ cm^3 and two iron blocks of dimensions $10 \times 20 \times 20$ cm^3 placed on a support structure 65 cm in the vertical direction. The 3D reconstruction of this layout is shown below on Figure 15.

The position of the blocks is reproduced correctly but there is finite spatial resolution in the reconstruction especially in the vertical direction. The reconstructed scattering density of the lead blocks is greater than that of the iron blocks. Its straightforward to discriminate low Z or medium Z materials from high Z materials using this method. The problem with this method is that discrimination between high Z materials denser than iron is more difficult because of the non- linearity in the reconstructed scattering density. This means that the muon momentum has to be measured as well to allow a better material

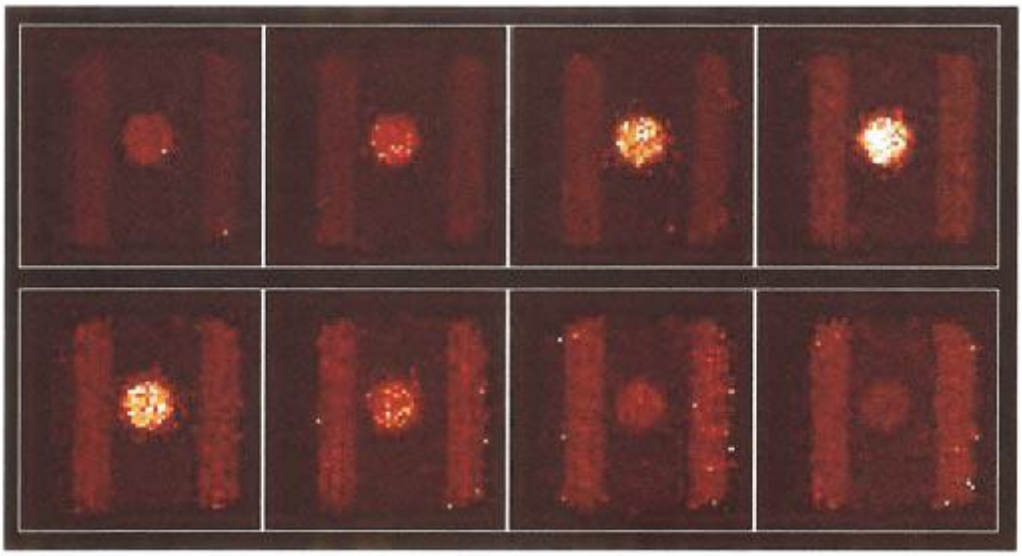

Figure 9: Test object reconstruction using 100 000 muons. A volumetric image of $1 \times 1 \times 1$ cm^3 voxels was reconstructed. The eight planes are horizontal slices near the middle of the volume, moving from top to bottom. Both the tungsten cylinder and the steel support beams are clearly visible. [5]

recognition and increase the statistical precision of the density measurement. [9]

3.3.7 Applications of muon tomography

Muon tomography could be used to protect the rail network from terrorism. The idea is to equip train stations with large muon detectors above and below. Density images can be produced very fast in a time scale of minutes. High density objects such as nail bombs and fissile materials will be easily identified. [10]

It could also be used as a detection method of nuclear devices or material in vehicles and containers. An automobile sized counting station could be used to scan vehicles at border crossing. This would allow examination of every vehicle and shipping container crossing a border. It will require enough detectors to handle the traffic at the borders. The total traffic crossing the US – Mexico and the US – Canada borders in 2008 was 1.3×10^8 vehicles. Assuming a single muon tomography detector could analyse a vehicle within 1 min and operates for 12 hours per day, then 500 detectors would be needed to handle the entire border crossing traffic. This would cost a total of 1.5 to 2 billion dollars but its negligible compared to the consequences of the detonation of a nuclear bomb. A picture of how it could be implemented at a border crossing is shown below on Figure 16. [8]

Both methods could be used for nuclear dismantlement verification. The vehicle transporting the bomb for disarmament could be scanned at several stations during its journey to the dismantlement facilities. A single muon tomography detector at the dismantlement facility could be used to verify a small

Figure 10: The Large Muon Tracker (LMT) prototype at the Los Alamos National Laboratory in 2006. The precise positions of muon tracks above and below the sampling region are determined by the overlapping X and Y detector planes. The new redundant detector planes will be used improve the tracking efficiency and quality. [7]

quantity of nuclear bombs. If there is a large number of bombs queued for verification then the idea of the train stations could be used. A room with muon detectors on the flood and the ceiling could be used to scan all of them at the same time.

Figure 11: Photograph of a car engine in the LMT at the Los Alamos National Laboratory in 2008. [8]

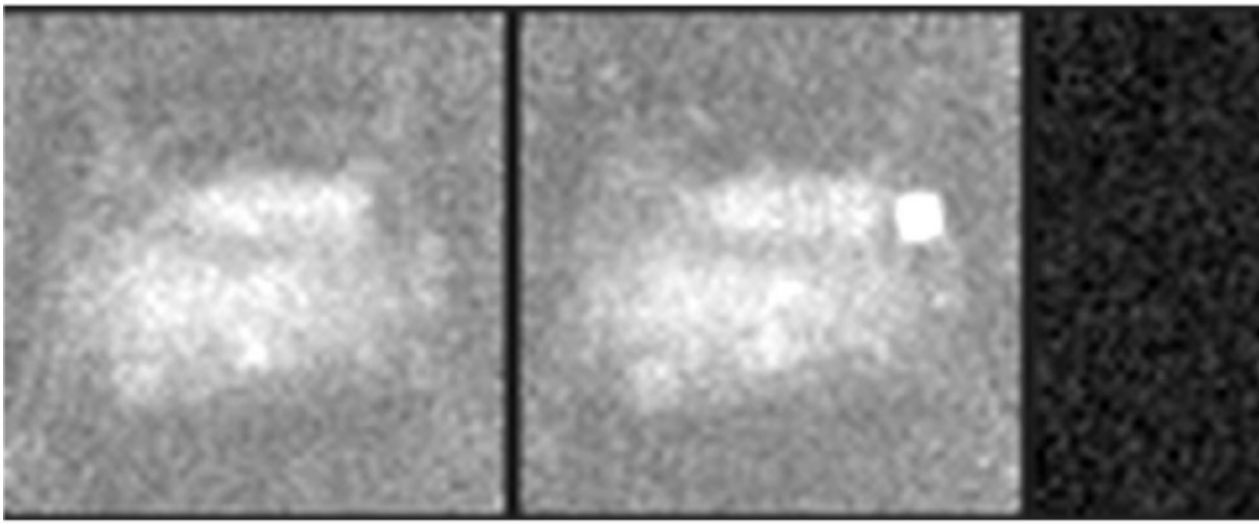

Figure 12: Mean scattering angle for a slice through the scene 50 cm above the base plate. The left image shows the car engine, the middle image shows the engine with the lead cube and the right image shows the difference of the other two images. The lead block stands out dramatically. [8]

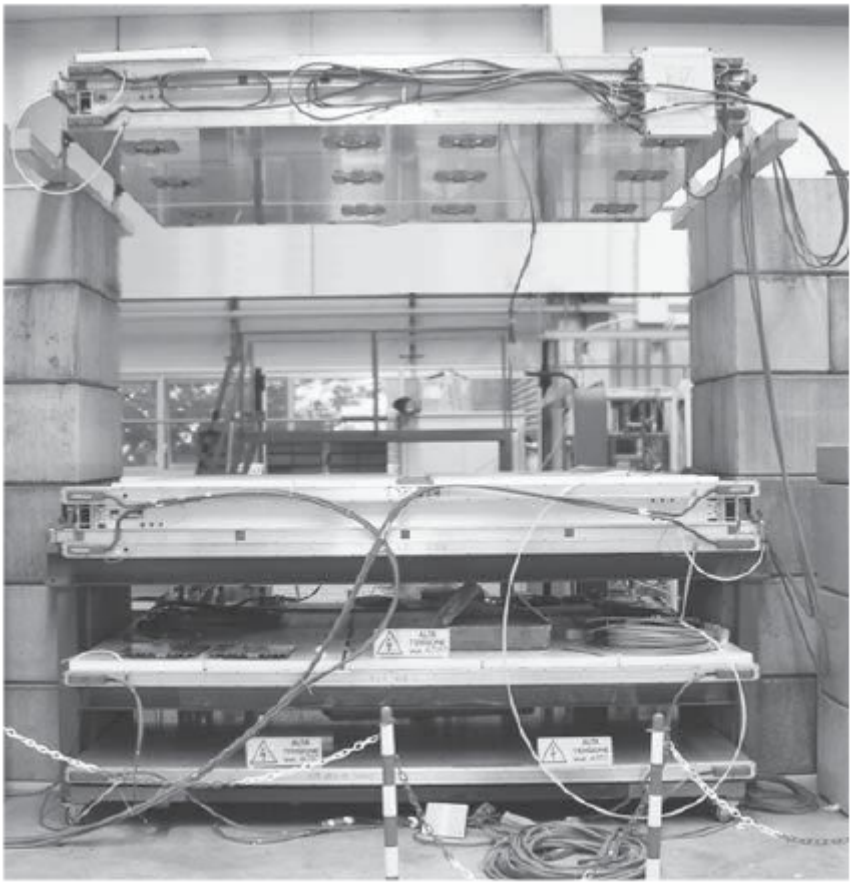

Figure 13: Muon tomography system prototype located at the INFN National Laboratories of Legnaro. [9]

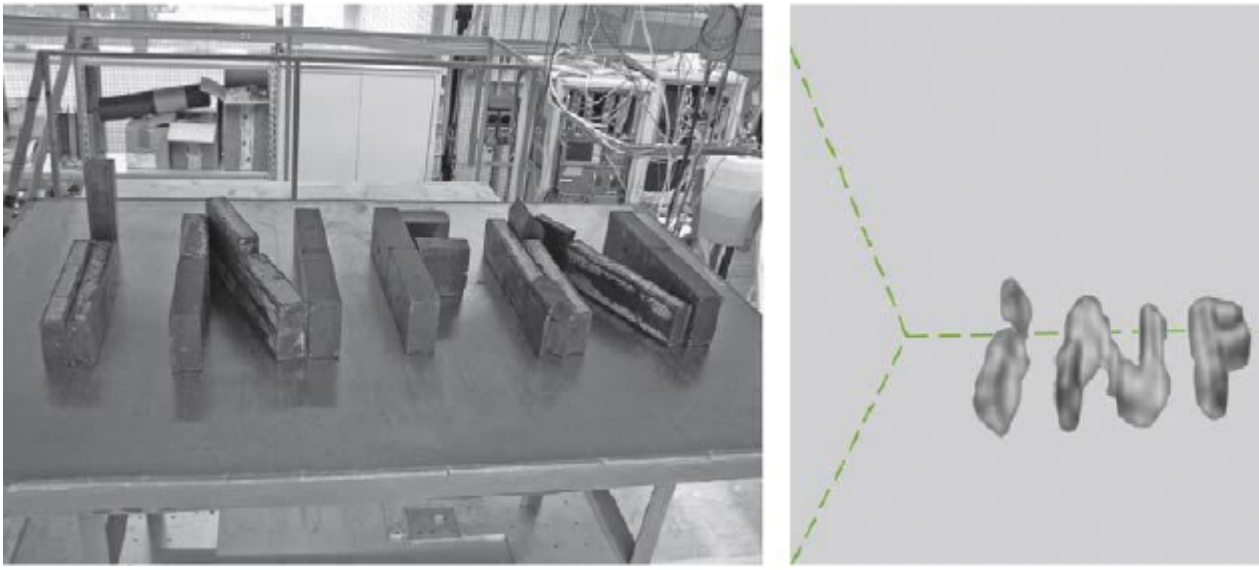

Figure 14: Test of the imaging capability of the prototype. The picture on the left shows the layout of iron bricks forming the word INFN and the picture on the right shows the result of the data analysis using the LMIA. The reconstructed image is very clear. [9]

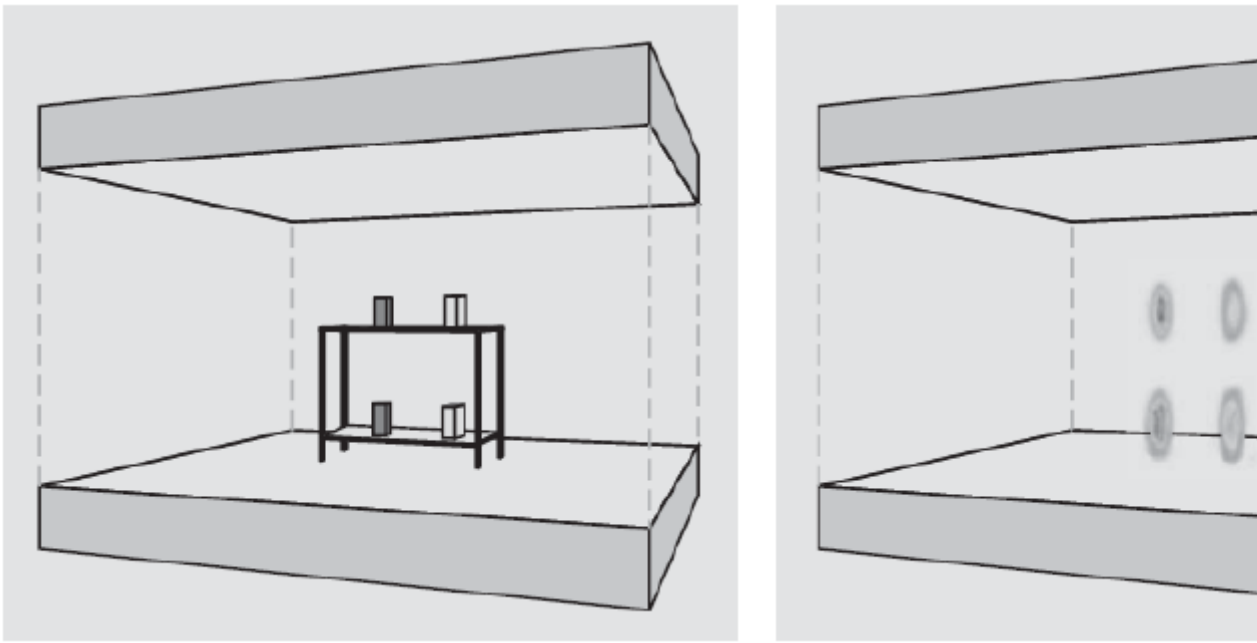

Figure 15: The left image is a sketch of the layout with the two lead and the two iron blocks. The darker blocks are the lead blocks. The right image shows the 3D view of the reconstructed image using the LMIA. [9]

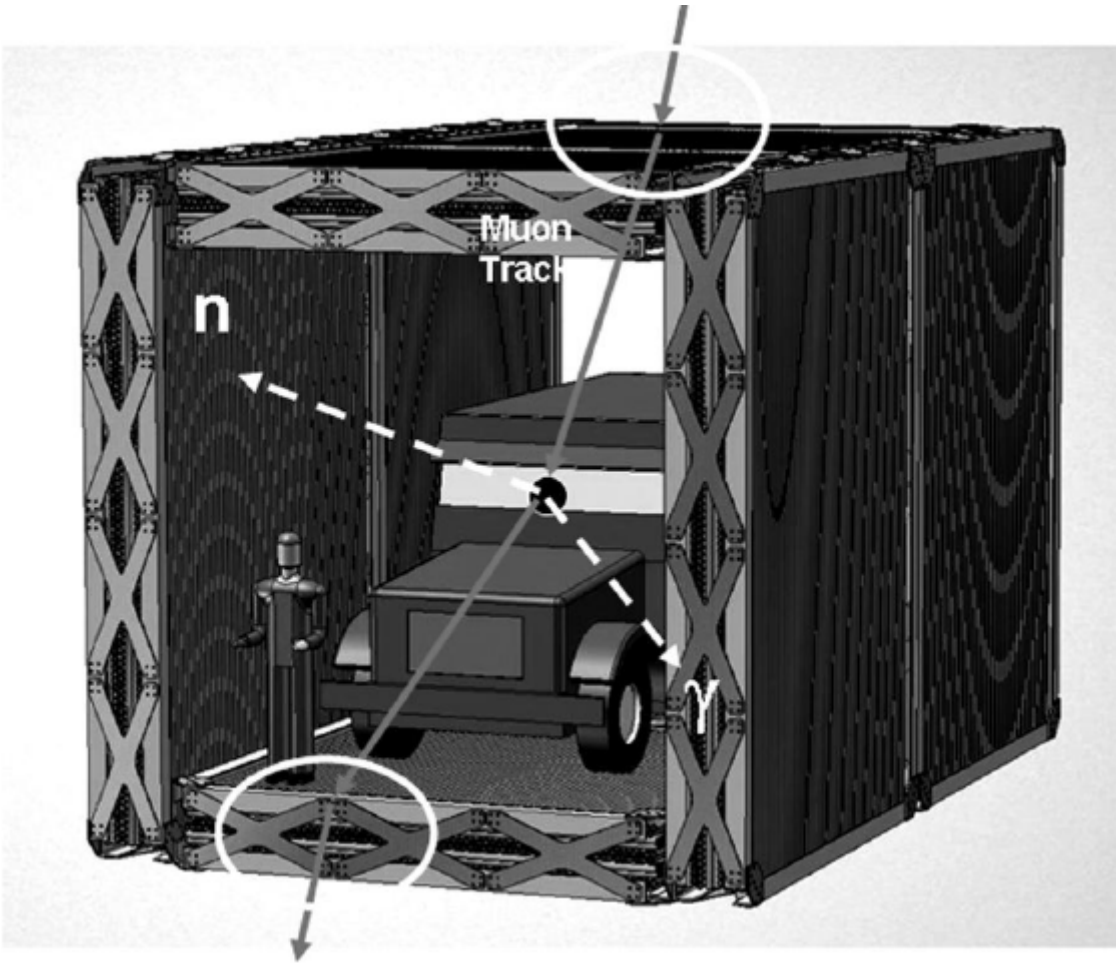

Figure 16: Schematic view of how a counting station might look. Vehicles would have to stop for approximately 20 seconds for the scan. [8]